



Detection and quantification of folic acid in serum via a dual-emission fluorescence nanoprobe

Yu He¹ · Shuo Wang² · Junping Wang¹

Received: 8 August 2019 / Accepted: 2 September 2019 / Published online: 11 September 2019
© Springer-Verlag GmbH Germany, part of Springer Nature 2019

Abstract

Folic acid (FA) is an essential vitamin in humans, and thus, rapid, accurate, and sensitive methods for its quantification in different biological samples are needed. This work describes a novel, simple, and effective dual-emission fluorescence nanoprobe for FA detection and quantification. The probe was covalently linked to amino-modified orange quantum dots (QDs) and carboxyl-modified blue graphene quantum dots (GQDs). The resulting material exhibited two emission peaks at 401 and 605 nm upon excitation at 310 nm. The probe had good selectivity and sensitivity toward FA with an exceptionally low detection limit (LOD = 0.09 nM). This probe was effectively used to quantify FA in animal serum samples. The method has potential utility for FA analysis in different types of biological samples.

Keywords Fluorescence · Dual-emission · Quantum dots · Folic acid · Rabbit serum

Introduction

Folic acid (FA) is a B-group vitamin essential for human and animal health. As a substrate and coenzyme, it participates in the metabolism of amino acids and nucleic acids via the addition, transport, and enzymatic treatment of one-carbon units [1, 2]. The deficiency of this vitamin increases the risk of cancer, cardiovascular disease, depression, cognitive decline, Alzheimer's disease, neural tube defects (NTD), and so on [3–7]. The free FA concentration in serum, plasma, and erythrocytes has been used as a biomarker for the effective diagnosis of a panel of health disorders [8]. FA is also very important for normal homeostasis. Thus, portable, rapid, simple, sensitive, accurate, and affordable methods for the detection and quantification of FA in biological samples are needed.

The current methods for FA determination are based on high-performance liquid chromatography (HPLC), capillary electrophoresis (CE), surface-enhanced Raman scattering

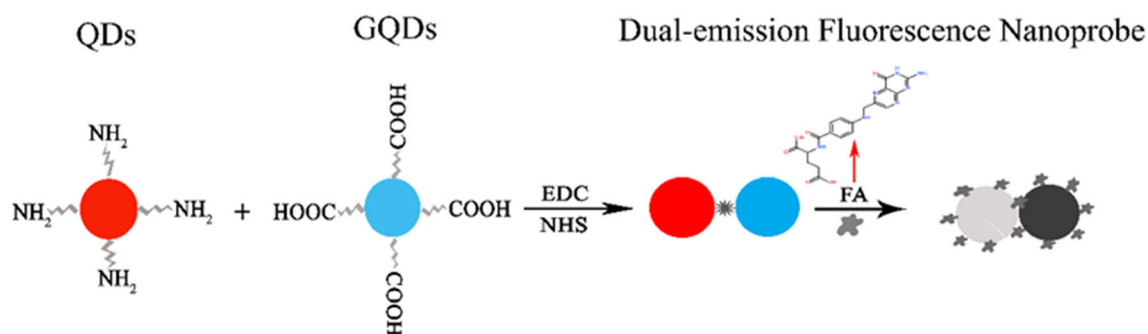
(SERS), electrochemistry, and ELISA [1, 3, 9–12]. Most of these methods require expensive equipment and complex sample preparation and analysis [13]. The detection of trace analytes by fluorescence spectroscopy is a potentially useful technique. Versus traditional methods, fluorescence spectroscopic technique is fast, simple, sensitive, and selective, making it attractive for a wide variety of practical applications. Quantum dots (QDs) are the most promising, inorganic nanomaterials in the analytical field due to their unique optical and physical characteristics, such as adjustable size, high quantum yield, large Stokes shifts, high optical stability, and high absorption coefficients [14–16]. In recent years, the number of applications using QDs as fluorescent-sensing probes has increased [17, 18]. The selectivity of the QDs is reduced when the sample matrix contains substances with a similar luminescence response as the analyte. To overcome this problem, radiometric fluorescence nanoprobe have been developed. The probe takes the intensity ratio at two emission wavelengths as the output signal. This signal is self-calibrated eliminating the interference originating from background and further improving the sensitivity, selectivity, and accuracy of detection [19–21].

Here, we designed and synthesized a novel, simple, and effective dual-emission fluorescence nanoprobe. The structure of the dual-emission fluorescence nanoprobe and the working principle for visual detection of FA are illustrated in Scheme 1. To design such a dual-emission fluorescence nanoprobe for

✉ Junping Wang
wangjp@tust.edu.cn

¹ State Key Laboratory of Food Nutrition and Safety, College of Biotechnology and Food Engineering, Tianjin University of Science and Technology, Tianjin 300457, China

² Tianjin Key Laboratory of Food Science and Health, School of Medicine, Nankai University, Tianjin 300071, China



Scheme 1 Synthesis of a dual-emission fluorescent nanoprobe and detection principle of FA

visual detection of FA, amino-modified orange QDs and carboxyl-modified blue graphene quantum dots (GQDs) are chemically combined through a condensation process and catalyzed by EDC/NHS. These materials show two emission peaks of 401 and 605 nm upon excitation at 310 nm. The free FA in solution quenched the fluorescence of the probe leading to a very low LOD (0.03 nM). This probe was successfully utilized for the quantification of FA in animal serum samples. The method is fast, simple, specific, and sensitive with potential applicability for different types of biological samples.

Synthesis of GQDs

The preparation was performed according to the previously described procedure [22]. Briefly, 2 g Ca and 0.5 g Tris-HMA were mixed in a 25-mL round-bottomed flask and heated at 225 °C for 15 min. The final product precipitated after cooling to room temperature. Next, 5 mL of ultrapure water was added with dissolved solids, pH was adjusted to 7, the salt was removed by overnight dialysis, and the GQDs were obtained and diluted to 50 mL for the experiment.

Materials and methods

Reagents and equipment

Anhydrous citric acid was bought from Sinopharm (Shanghai, CHN). Tris (hydroxymethyl) aminomethane (Tris-HMA), NaOH, FA, EDC, and NHS were purchased from Aladdin (Shanghai, CHN). Water-soluble amino-modified QDs (CdSe/ZnS) were bought from ZhongKeWuYuan Biotechnology (Beijing, CHN).

The UV-Vis, FL, and Fourier-transform infrared (FT-IR) spectra were recorded on a UV-Cary50 Bio (Victoria, Australia), Lumina FL-4500 (Thermo Fisher, America), and Vector-22 (Bruker, Germany), respectively.

Synthesis of dual-emission fluorescent nanoprobe

A dual-emission nanoprobe was synthesized by covalent coupling between amino-modified orange QDs and carboxyl-modified blue GQDs [23–25]. The specific steps were as follows: First, 50 μL of GQDs and 30 μL of 1 mg/mL EDC/NHS were added in 1.5-mL centrifuge tubes and shaken for 15 min to activate the carboxylic groups. Afterward, 200 μL of QDs and 720 μL of 10 nM PBS (pH = 7.4) were supplemented, and the reaction proceeded in the dark for 24 h. After centrifugation to remove an excess of unreacted compounds, the synthesized dual-emission fluorescence nanoprobe was kept for further use as dispersion in 1 mL PBS.

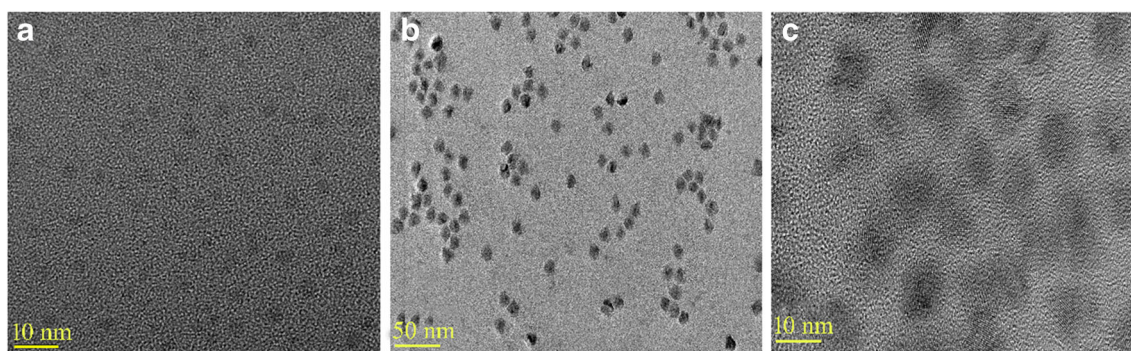


Fig. 1 **a** TEM diagram of GQDs. Bar = 10 nm. **b** TEM diagram of dual-emission fluorescence nanoprobe. Bar = 50 nm. **c** TEM diagram of QDs. Bar = 10 nm

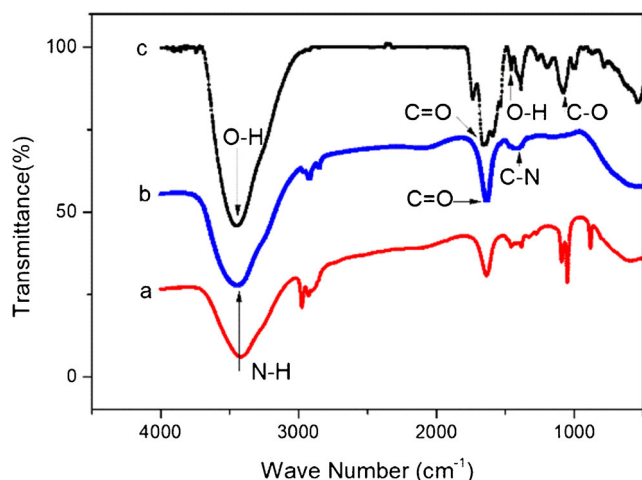


Fig. 2 FT-IR spectra of (a) QDs, (b) dual-emission fluorescence nanoprobe, and (c) GQDs

Fluorescence detection of FA

Briefly, 20 μL of dual-emission fluorescence nanoprobe was diluted with PBS and mixed with the increasing amounts of FA. The final concentrations of FA in the mixtures were 0.11, 0.22, 1.13, 2.27, 4.53, 11.33, and 22.66 nM while keeping the sample volume constant (1 mL). Upon excitation at 310 nm, emission signal from FA was detected at 401 and 605 nm (at room temperature). Experiments were performed at least in triplicate using biological samples.

Selectivity of probes toward FA

The fluorescence intensity at 401 and 605 nm was measured after mixing the dual-emission fluorescence nanoprobe with the interfering substance and adding 100 μL of 22.66 nM FA

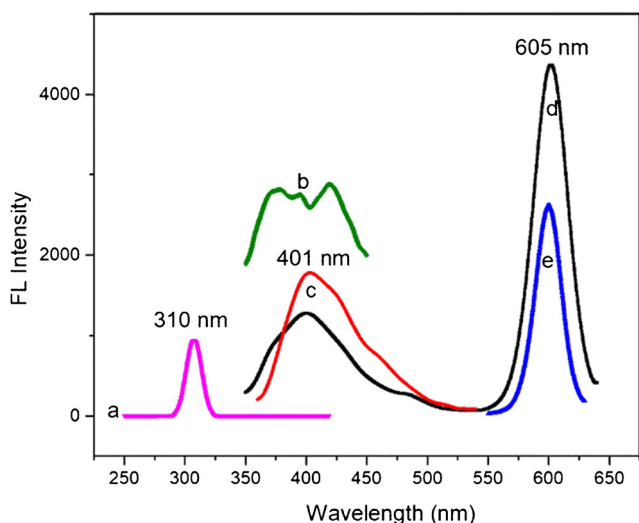


Fig. 3 (a) Fluorescence excitation spectra of the dual-emission fluorescence nanoprobe. (b) Fluorescence excitation spectra of QDs. (c) Emission spectra of GQDs. (d) Emission spectra of the dual-emission fluorescence nanoprobe. (e) Emission spectra of the QDs

solution. In the presence of FA, the other substances from the biological matrix such as carbohydrates, amino acids, and metal ions were separately introduced into the nanoprobe solution to investigate the selectivity.

Detection of FA in rabbit serum samples

The rabbit serum used in the experiment was purchased from the BioChannel Company (Nanjing, PRC. Cat: BC-SE-RAB001-100 ml, Lot: BC20190110), being kept at $-20\text{ }^{\circ}\text{C}$. The serum samples were diluted 200 times with ultrapure water because of the high FA content in rabbit serum. The standard recovery of FA was determined by adding increasing amounts of analyte into the diluted serum samples.

Results and discussion

Characterization

TEM diagrams of GQDs and dual-emission fluorescence nanoprobe are shown in Fig. 1. Figure 1a and c show that GQDs and QDs were uniformly dispersed in water. Along with this, two types of QDs are successfully connected by chemical forces and dispersed densely and uniformly in an aqueous solution.

The FT-IR absorption spectra of GQDs, QDs, and dual-emission fluorescence nanoprobe are shown in Fig. 2. GQDs and QDs were coupled by amide bonds formed between amino and carboxyl groups. The hydroxyl and carboxyl groups existed on the surface of GQDs (Fig. 2(c)). The absorption maxima at 1456 cm^{-1} and 3446 cm^{-1} indicate in-plane bending and stretching vibrations of the O-H group, respectively [26]. The absorption peaks at 1662 cm^{-1} and 1078 cm^{-1} arise from C=O and C-O stretching vibrations, respectively. The

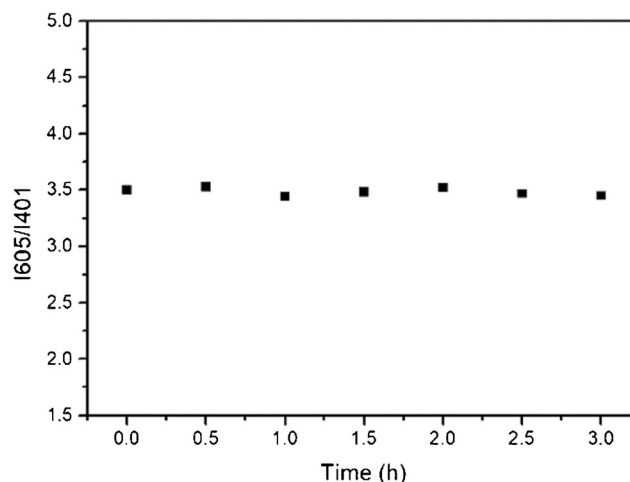


Fig. 4 Stability of the fluorescence intensity of the dual-emission fluorescence nanoprobe for 3 h

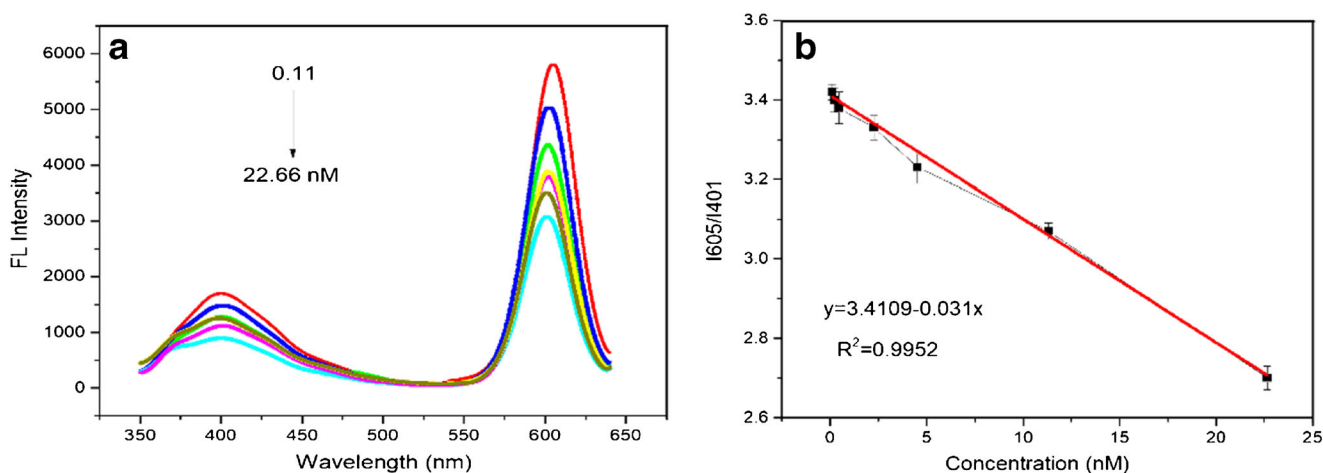


Fig. 5 **a** Emission spectra of the dual-emission fluorescence nanoprobe upon addition of increasing amounts of FA. **b** The linear dependence of fluorescence intensity ratio (I_{605}/I_{401}) and FA concentration

characteristic peaks of amino functional groups are observed at the surface of QDs. The most intense absorption peaks at 3421 cm^{-1} (Fig. 2(a)) and 3450 cm^{-1} (Fig. 2(b)) were assigned to N-H stretching vibrations; signals at 1640 cm^{-1} and 1400 cm^{-1} originate from of the C=O stretching vibrations (Fig. 2(b)). This confirms the formation of amide bonds in the dual-emission fluorescence nanoprobe.

Optical properties

The fluorescence spectrum emissions of blue-emitting QDs, orange-emitting QDs, and dual-emission fluorescence

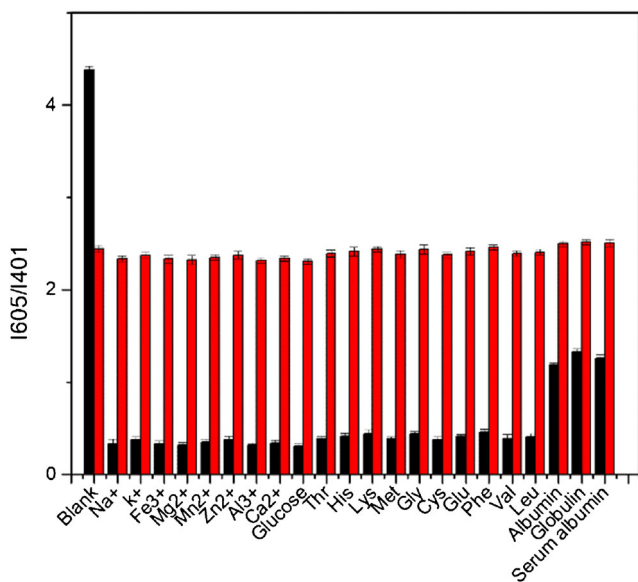


Fig. 6 The fluorescence response of the dual-emission fluorescence nanoprobe to interferences. The black bars indicate the fluorescence signal upon addition of $0.1\text{ }\mu\text{M}$ metal ions (Na^+ , K^+ , Mg^{2+} , Mn^{2+} , Zn^{2+} , Al^{3+} , Ca^{2+} , and Fe^{3+}), glucose, amino acids (Thr, His, Lys, Met, Gly, Cys, Glu, Phe, Val, and Leu), and protein (albumin, globulin, serum albumin). The red bars represent the signal from 10 nM FA added to each of the above solutions

nanoprobe are shown in Fig. 3. The wavelength of QDs' fluorescence maximum emission is 401 nm , while QDs show a maximum emission peak at 605 nm . Upon excitation at 310 nm , the blue-emitting QDs and orange-emitting QDs emitted intense blue and red fluorescence at 401 and 605 nm , respectively, which indicates that the functional groups of QDs and QDs have been successfully bonded.

Fluorescence stability

Fluorescence stability is an important parameter that indicates whether the synthetic sensing material can be used in practical detection. Stable fluorescence signal ensures the accuracy and repeatability of the measurements. Therefore, we monitored the stability of the dual-emission fluorescence nanoprobe emission in an aqueous solution. The fluorescence emission spectrum was measured every 30 min for 3 h . Figure 4 shows that the ratio of fluorescence at two wavelengths remained nearly constant for 3 h , indicating good stability of the dual-emission fluorescence nanoprobe in solution. This makes it suitable for daily analysis and detection.

Fluorescence sensing of FA using the emission intensity ratio at two wavelengths

The sensitivity of the dual-emission fluorescence nanoprobe toward FA was investigated next (Fig. 5). The fluorescence spectra of the dual-emission fluorescence nanoprobe in the presence of different amounts of FA were recorded. Figure 5a shows that the fluorescence intensity at 401 and 605 nm decreased with FA concentration. The fluorescence intensity ratio depends linearly on the FA concentration from 0.11 - to 22.66-nM range (Fig. 5b). Linear regression analysis showed $I_{605}/I_{401} = 3.4109 - 0.031 \times \text{Concentration}$ with a correlation coefficient $r = 0.9952$. The detection limit (LOD) was 0.09 nM according to the formula $\text{LOD} (S/N = 3\sigma/k)$ [27],

Table 1 Quantification of FA in rabbit serum by a dual-emission fluorescence nanoprobe

Sample	Add (nM)	Found (nM)	Recovery (%)	RSD (%)
Rabbit serum sample 1	0	11.33 ± 0.13	–	0.97
	1	12.31 ± 0.22	98.7 ± 1.9	1.94
	2	13.33 ± 0.1	99.9 ± 2.4	1.06
	3	14.32 ± 0.17	99.7 ± 2.0	2.37
Rabbit serum sample 2	0	24.92 ± 0.51	–	4.26
	1	25.9 ± 0.54	98.5 ± 2.6	4.63
	2	26.86 ± 0.47	97.2 ± 3.1	3.25
	3	27.78 ± 0.39	95.6 ± 3.4	4.07

where σ is the standard deviation of the response and k is the slope of the calibration curve. These results proved the high selectivity, wide linear range, and low detection limit for the detection and quantification of FA using a novel dual-emission fluorescence nanoprobe. This makes it suitable as a sensing material for FA analysis.

Selectivity and potential interferences for FA analysis using a dual-emission fluorescence nanoprobe

Biological samples have a complex matrix, and evaluating potential interferences is an essential step in the development of FA sensors. To evaluate the selectivity of this dual-emission fluorescence nanoprobe toward FA, the fluorescence reaction of the probe was studied in the presence of competing analytes such as glucose, protein, amino acids (Thr, His, Lys, Met, Gly, Cys, Glu, Phe, Val, and Leu), metal ions (Na⁺, K⁺, Mg²⁺, Mn²⁺, Zn²⁺, Al³⁺, Ca²⁺, and Fe³⁺), and protein (albumin, globulin, serum albumin). After further addition of 10 nM FA, the fluorescence intensity ratio (I_{605}/I_{401}) of the probe changes greatly, even when it coexists with the interferences whose concentrations (0.1 μM) are at least 10 times than those of FA. The fluorescence spectrum was measured under the same conditions and the I_{605}/I_{401} value slot tally was calculated. As shown in Fig. 6, under the same detection conditions, only FA shows a significant fluorescence response compared

with blank samples, with the maximum increase in the I_{605}/I_{401} value. Since the interference ions do not have a significant corresponding fluorescence to the probe at a concentration higher than FA, it reflects the high selectivity of the probe against the FA. Thus, the dual-emission fluorescence nanoprobe had good specificity toward FA and low interference in the presence of biological matrix substances.

Quenching mechanism of the dual-emission fluorescence nanoprobe

In order to accurately judge the quenching mechanism of QDs, the zeta potential of QDs and FA in PBS buffer solution was measured. The zeta potentials of QDs and FA were –40.8 mV and +9.07 mV, respectively. The results showed that the surface of QDs was negatively charged while the surface of FA was positively charged, so it could be speculated that there was a strong electrostatic interaction between QDs and FA [28, 29]. FA was adsorbed to the surface of QDs by electrostatic interaction, and finally, the fluorescence quenching of QDs was caused by charge transfer [28–31].

However, the absorption spectrum of FA does not overlap with the emission spectra of GQDs—there was no potential for FRET between FA and GQDs. FA can decay the radiative emission of GQDs because the polar functional groups (-OH, -COOH, and -NH₂) of FA can establish hydrogen-bonding

Table 2 The linear range and LOD for different methods developed for FA analysis

Method	Linear range (μM)	LOD (μM)	Reference
Fluorescence	0.5–200	0.18	[34]
Fluorescence	0.2–100	0.08	[35]
Cyclic voltammetry	1.0 × 10 ⁻³ –44.0 × 10 ⁻³	0.12 × 10 ⁻³	[36]
Capillary electrophoresis	12.0–48.0	0.612	[37]
ELISA	0.36 × 10 ³ –2.90 × 10 ³	40.78	[2]
Surface-enhanced Raman scattering	0.5–25.0	0.3	[11]
Fluorescence	0.01–30	0.5 × 10 ⁻³	[38]
Fluorescence	0.11 × 10 ⁻³ –22.66 × 10 ⁻³	0.03 × 10 ⁻³	This work

interactions with -OH and -COOH groups on the surface of QGDs leading to fluorescence quenching of carbon dots [22, 32, 33].

Detection of FA in animal serum

Because of the high FA content in rabbit serum, the serum samples were diluted 200-fold to fall into the calibration curve, which underscores the excellent sensitivity of this method. The standard recovery of FA was determined by adding increasing amounts of analyte into the diluted serum samples. The 200-fold diluted rabbit serum samples contained 11.33–24.92 nM of FA (Table 1). In addition, the recovery rate of FA in the standard recovery experiment was 95.6–99.9%, while the relative standard deviation (RSD) was below 5%. Therefore, this newly developed dual-emission fluorescence nanoprobe was suitable for quantification of FA in animal serum, and the newly developed method might be applicable to biological samples.

Comparison with reported methods

This method had very low detection limits and high sensitivity (Table 2), making it an interesting candidate for practical detection and quantification of FA in real samples.

Conclusion

In this work, we developed a novel dual-emission fluorescence nanoprobe chemically linked to orange and blue quantum dots. This probe exerts dual-wavelength emission via single-wavelength excitation. The main advantages of this probe are its wide linear range, high sensitivity, and good selectivity. Compared with traditional methods, this probe offers rapid determination and quantification of FA with a detection limit below all other competing methods. It has utility in serum samples and thus has a great potential for practical applications.

Acknowledgments We thank LetPub (www.letpub.com) for its linguistic assistance during the preparation of this manuscript.

Funding information This work was supported by “The National Key R&D Program of China” (No. 2016YFD0401202) and the Special Project of Tianjin Innovation Platform (No. 17PTGCCX00230).

Compliance with ethical standards

Conflict of interest The authors declare that they have no competing interests.

References

- Lermo A, Fabiano S, Hernandez S, Galve R, Marco M-P, Alegret S, et al. Immunoassay for folic acid detection in vitamin-fortified milk based on electrochemical magneto sensors. *Biosens Bioelectron.* 2009;24(7):2057–63.
- Hoegger D, Morier P, Vollet C, Heini D, Reymond F, Rossier JS. Disposable microfluidic ELISA for the rapid determination of folic acid content in food products. *Anal Bioanal Chem.* 2007;387(1):267–75.
- Zhao SL, Yuan HY, Xie C, Xiao D. Determination of folic acid by capillary electrophoresis with chemiluminescence detection. *J Chromatogr A.* 2006;1107(1–2):290–3.
- Jiang XL, Li R, Li J, He X. Electrochemical behavior and analytical determination of folic acid on carbon nanotube modified electrode. *Russ J Electrochem.* 2009;45(7):772–7.
- Iyer R, Tomar SK. Folate: a functional food constituent. *J Food Sci.* 2009;74(9):114–22.
- Chew SC, Loh SP, Khor GL. Determination of folate content in commonly consumed Malaysian foods. *Int Food Res J.* 2012;19(1):189–97.
- Wang M, Niu W, Wu X, Li L, Yang J, Shuang S, et al. Fluorescence enhancement detection of uric acid based on water soluble 3-mercaptopropionic acid capped core/shell ZnS:Cu/ZnS. *RSC Adv.* 2014;4:25183–8.
- Chakravarty S, Dutta P, Kalita S, Sarma NS. PVA-based nanobiosensor for ultrasensitive detection of folic acid by fluorescence quenching. *Sensors Actuators B Chem.* 2016;232:243–50.
- Breithaupt DE. Determination of folic acid by ion-pair RP-HPLC in vitamin-fortified fruit juices after solid-phase extraction. *Food Chem.* 2001;74(4):521–5.
- Pawlosky RJ, Flanagan VP. A quantitative stable-isotope LC-MS method for the determination of folic acid in fortified foods. *J Agric Food Chem.* 2001;49(3):1282–6.
- Ren W, Fang YX, Wang E. A binary functional substrate for enrichment and ultrasensitive SERS spectroscopic detection of folic acid using graphene oxide/Ag nanoparticle hybrids. *ACS Nano.* 2011;5(8):6425–33.
- Kalimuthu P, Abraham JS. Selective electrochemical sensor for folic acid at physiological pH using ultrathin electropolymerized film of functionalized thiadiazole modified glassy carbon electrode. *Biosens Bioelectron.* 2009;24(12):3575–80.
- Chen ZG, Zhang GM, Chen X, Chen JH, Liu JB, Yuan HQ. A fluorescence switch sensor for 6-mercaptopurine detection based on gold nanoparticles stabilized by biomacromolecule. *Biosens Bioelectron.* 2013;41:844–7.
- Alivisatos AP. Semiconductor clusters, nanocrystals, and quantum dots. *Science.* 1996;271(5251):933–7.
- Smith AM, Nie S. Semiconductor nanocrystals: structure, properties, and band gap engineering. *Acc Chem Res.* 2010;43(2):190–200.
- Genger UR, Grabolle M, Nitschke R, Nann T. Nanocrystals and nanoparticles versus molecular fluorescent labels as reporters for bioanalysis and the life sciences: a critical comparison. *Advanced Fluorescence Reporters in Chemistry and Biology II.* 2010;03:3–40.
- Tyrakowski CM, Preston TS. Ratiometric CdSe/ZnS quantum dot protein sensor. *Anal Chem.* 2014;86(5):2380–6.
- Qu ZB, Zhou XG, Gu L, Lan R, Sun D, Yua D, et al. Boronic acid functionalized graphene quantum dots as a fluorescent probe for selective and sensitive glucose determination in microdialysate. *Chem Commun.* 2013;49:9830–2.
- Shao N, Jin JY, Wang H, Zhang Y, Yang RH, Chan WH. Tunable photochromism of spirobenzopyran via selective metal ion

- coordination: an efficient visual and ratioing fluorescent probe for divalent copper ion. *Anal Chem.* 2008;80(9):3466–75.
20. Wang M, Mei QS, Zhang K, Zhang ZP. Protein-gold nanoclusters for identification of amino acids by metal ions modulated ratiometric fluorescence. *Analyst.* 2012;137(7):1618–23.
 21. Zhang K, Zhou HB, Mei QS, Wang SH, Guan GJ, Liu RY, et al. Instant visual detection of trinitrotoluene particulates on various surfaces by ratiometric fluorescence of dual-emission quantum dots hybrid. *J Am Chem Soc.* 2011;133(22):8424–7.
 22. Lin LP, Rong MC, Lu SS, Song XH, Zhong YX, Yan JW, et al. Facile synthesis of highly luminescent nitrogen-doped graphene quantum dots for the detection of 2,4,6-trinitrophenol in aqueous solution. *Nanoscale.* 2015;7(5):1872–8.
 23. Conde J, Bao C, Cui D, Baptista PV, Tian F. Antibody-drug gold nanoantennas with Raman spectroscopic fingerprints for in vivo tumour theranostics. *Control Release.* 2014;183(10):87–93.
 24. Krishnamoorthy G, Selvakumar R, Sastry TP, Sadulla S, Mandal AB, Doble M. Experimental and theoretical studies on Gallic acid assisted EDC/NHS initiated crosslinked collagen scaffolds. *Mater Sci Eng C.* 2014;43:164–71.
 25. Wang YH, Zhang C, Chen XC, Yang B, Yang L, Jiang CL, et al. Ratiometric fluorescent paper sensor utilizing hybrid carbon dots quantum dots for the visual determination of copper ions. *Nanoscale.* 2016;8(11):5977–84.
 26. Li X, Zhao Z. Facile ionic-liquid-assisted electrochemical synthesis of size-controlled carbon quantum dots by tuning applied voltages. *RSC Adv.* 2014;101(4):57615–9.
 27. Wang YH, Zhang C, Chen XC, Yang B, Yang L, Jiang CL, et al. Ratiometric fluorescent paper sensor utilizing hybrid carbon dots–quantum dots for the visual determination of copper ions. *Nanoscale.* 2016;00:1–3.
 28. Bai WJ, Zheng ZH, Long YJ, Mao XJ, Gao M, Zheng LY. A carbon dots-based fluorescence turn-on method for DNA determination. *Anal Sci.* 2011;27:243–6.
 29. Callan JF, Mulrooney RC, Kamila S. Luminescent detection of ATP in aqueous solution using positively charged CdSe-ZnS quantum dots. *J Fluoresc.* 2008;18(6):1157–61.
 30. Lee JH, Choi YS, Kim JW, Park EJ, Song R. Positively charged compact quantum dot–DNA complexes for detection of nucleic acids. *Chem Phys Chem.* 2009;10:806–11.
 31. Liu YS, Zhao YN, Zhang YY. One-step green synthesized fluorescent carbon nanodots from bamboo leaves for copper(II) ion detection. *Sensors Actuators B.* 2014;196:647–52.
 32. Yang M, Li H, Liu J, Kong WQ, Zhao SY, Li CX, et al. Convenient and sensitive detection of norfloxacin with fluorescent carbon dots. *J Mater Chem B.* 2014;45(2):7964–70.
 33. Ratajczak K, Krazinski BE, Kowalczyk AE, Dworakowska B, Jakiela S, Stobiecka M. Optical biosensing system for the detection of survivin mRNA in colorectal cancer cells using a graphene oxide carrier-bound oligonucleotide molecular beacon. *Nanomaterials.* 2018;8:510.
 34. Li XG, Wu XM, Zhang F, Zhao B, Li Y. Label-free detection of folic acid using a sensitive fluorescent probe based on ovalbumin stabilized copper nanoclusters. *Talanta.* 2019;195(1):372–80.
 35. Liu PF, Liu D, Liu YH, Li L. ANTS-anchored Zn-Al-CO₃-LDH particles as fluorescent probe for sensing of folic acid. *J. Sol State Chem.* 2016;241:164–72.
 36. Gujska E, Kuncewicz A. Determination of folate in some cereals and commercial cereal-grain products consumed in Poland using trienzyme extraction and high performance liquid chromatography methods. *Eur Food Res Technol.* 2005;221(1–2):208–13.
 37. Uysal UD, Oncu-Kaya EM, Tuncel M. Determination of folic acid by CE in various cultivated variety of lentils. *Chromatographia.* 2010;71(7–8):653–8.
 38. Wang M, Jiao Y, Cheng CS, Hua JH, Yang YL. Nitrogen-doped carbon quantum dots as a fluorescence probe combined with magnetic solid-phase extraction purification for analysis of folic acid in human serum. *Anal Bioanal Chem.* 2017;409(30):7063–75.

Publisher's note Springer Nature remains neutral with regard to jurisdictional claims in published maps and institutional affiliations.